Control Engineering Practice 27 (2014) 1–10

Contents lists available at ScienceDirect

Control Engineering Practice

journal homepage: www.elsevier.com/locate/conengprac

Extended complex Kalman filter for sensorless control of an induction motor

Francesco Alonge*, Filippo D'Ippolito, Adriano Fagiolini, Antonino Sferlazza

Dipartimento di Energia, Ingegneria dell'Informazione e Modelli Matematici (DEIM), Faculty of Engineering, University of Palermo, Italy

ARTICLE INFO

Article history:
Received 26 April 2013
Accepted 7 February 2014

Keywords:
Induction motor
Observability
Kalman filtering
Complex-valued model

ABSTRACT

This paper deals with the design of an extended complex Kalman filter (ECKF) for estimating the state of an induction motor (IM) model, and for sensorless control of systems employing this type of motor as an actuator. A complex-valued model is adopted that simultaneously allows a simpler observability analysis of the system and a more effective state estimation. The observability analysis of this model is first performed by assuming that a third order ECKF has to be designed, by neglecting the mechanical equation of the IM model, which is a valid hypothesis when the motor is operated at constant rotor speed. It is shown that this analysis is more effective and easier than the one performed on the corresponding real-valued model, as it allows the observability conditions to be directly obtained in terms of stator current and rotor flux complex-valued vectors. Necessary observability conditions are also obtained along with the well-known sufficient ones. It is also shown that the complex-valued implementation allows a reduction of 35% in the computation time w.r.t. the standard real-valued one, which is obtained thanks to the lower dimensions of the matrices of the ECKF w.r.t. the ones of the real-valued implementation and the fact that no matrix inversion is required. The effectiveness of the proposed ECKF is shown by means of simulation in Matlab/Simulink environment and through experiments on a real low-power drive.

1. Introduction

Sensorless control of systems employing induction motors as actuators requires the estimation of the rotor speed together with the rotor flux components that cannot be directly measured. The estimation of the IM rotor speed can be performed by means of two types of methods, both exploiting the information from stator current measurement. The former type of method is based on the recognition of the characteristics (Holtz, 2002; Hurst & Habetler, 1996) of the measured currents, whereas the latter one is a model-based approach (Rajashekara, Kawamura, & Matsuse, 1996; Vas, 1998). The first type of methods can be invasive if based on the superimposition of suitable signals to the standard ones (Holtz, 2002), but not invasive if based on spectral analysis of the stator currents (Hurst & Habetler, 1996). They are also subject to interpretation errors of the above characteristics. The second type of methods use a priori knowledge of the actual system and are not invasive since they involve only measured variables. Moreover, their sensitivity to variations of the model's parameters or poor knowledge of their values can be countered by using robust estimation techniques. Among these model-based methods, MRAS-type (Cirrincione, Pucci, Cirrincione, & Capolino, 2004; Tajima & Hori, 1993), Luenberger-type (Cirrincione, Pucci, Cirrincione, & Capolino, 2006; Rajashekara et al., 1996), and sliding mode observers (Ghanes & Zheng, 2009; Rodic & Jezernik, 2002; Yan, Jin, & Utkin, 2000) are good examples of deterministic observers, whereas Kalman filters (Alonge, D'Ippolito, & Sferlazza, 2014) and extended Kalman filters (Alonge & D'Ippolito, 2010; Kim, Sul, & Park, 1994; Vas, 1998) are good examples of stochastic estimators.

In this paper the problem of designing a state observer for the IM consisting of an extended complex-valued Kalman filter is addressed, based on a complex-valued description of the dynamical behavior of the IM itself (cf. Menaa, Touhami, Ibtiouen, & Fadel, 2007; Petersen & Savkin, 1999; Vas, 1998). The model in question is of reduced order with state variables given by the complex stator current, the complex rotor flux, and a real variable representing the rotor speed. Related to the possibility of building such a state observer is the study of the observability property of the complex-valued model. In the standard real-valued framework this property has been largely studied since the seminal work of Canudas De Wit, Youssef, Barbot, Martin, and Malrait (2000) and later in Marino, Tomei, and Verrelli (2010), Ibarra-Rojas, Moreno, and Espinosa-Pérez (2004), and Ghanes, De Leon, and Glumineau

* Corresponding author.
E-mail addresses: francesco.alonge@unipa.it (F. Alonge), filippo.dippolito@unipa.it (F. D'Ippolito), adriano.fagiolini@unipa.it (A. Fagiolini), antonino.sferlazza@unipa.it (A. Sferlazza).

http://dx.doi.org/10.1016/j.conengprac.2014.02.007
0967-0661

(2006). When assuming a constant rotor speed, the adoption of the complex-valued model allows us to derive necessary observability conditions, directly obtained in terms of stator current and rotor flux complex variables, along with the well-known sufficient ones obtained for the real-valued IM model (Canudas De Wit et al., 2000; Marino et al., 2010).

Furthermore, it is shown that the sufficient conditions, ensuring the observability property of the continuous-time complex-valued IM model, are preserved by a first-order Euler discretization, which is essential to prove the feasibility of a discrete-time estimator. To this regard, the use of extended Kalman filters for state estimation of real-valued IM models, even in speed sensorless configuration, is a well recognized approach (see e.g. Alonge & D'Ippolito, 2010; Kim et al., 1994). Recently, techniques allowing the optimization of the parameters of such filters have been proposed, based on deterministic (Alonge & D'Ippolito, 2010) as well as stochastic approaches (Buyamin, 2007). From a complexity viewpoint, the proposed ECKF allows the implementation of a state observer with a substantial reduction (around 35%) of the required computation time. This reduction is achieved since all involved matrices have lower dimensions than those obtained from the corresponding real-valued models, and no matrix inversion is needed as the system output is a scalar variable represented by the complex-valued stator current. Moreover, the ability of our ECKF to produce accurate estimates of the IM state is shown by means of simulation in Matlab/Simulink environment. Its practical applicability is successfully tested by means of experiments on a real low power drive, where the output of the filter is given to a simple proportional–integral controller.

The paper is organized as follows. Section 2 describes the complex-valued model of the IM. Section 3 deals with observability analysis of the model and provides necessary and sufficient observability conditions for it. Section 4 shows that the sufficient observability conditions are preserved under time-discretization. Section 5 describes the ECKF. Section 6 shows simulation results of a sensorless closed loop control system in which the estimator consists of an ECKF. Finally, Section 7 presents the experimental results, which shows the effectiveness of the proposed ECKF.

2. Complex model of the induction motor

As is well known, the standard mathematical model of the IM in stationary frame is given by

$$\dot{i}_\alpha = -a_{11} i_\alpha + a_{12}\psi_\alpha + f_1\psi_\beta\omega + f_1 u_\alpha, \tag{1}$$

$$\dot{i}_\beta = -a_{11} i_\beta + a_{12}\psi_\beta - f_1\psi_\alpha\omega + f_1 u_\beta, \tag{2}$$

$$\dot{\psi}_\alpha = a_{21} i_\alpha - a_{22}\psi_\alpha - \psi_\beta\omega, \tag{3}$$

$$\dot{\psi}_\beta = a_{21} i_\beta - a_{22}\psi_\beta + \psi_\alpha\omega, \tag{4}$$

$$\dot{\omega} = -a_{33}\omega - f_3(i_\alpha\psi_\beta - i_\beta\psi_\alpha) - g_5 t_l, \tag{5}$$

where

$$a_{11} = \frac{1}{L_e}\left(R_s + \frac{L_s - L_e}{\tau_r}\right), \quad a_{12} = \frac{1}{\tau_r L_e}, \quad a_{21} = \frac{L_s - L_e}{\tau_r},$$
$$a_{22} = \frac{1}{\tau_r}, \quad a_{33} = \frac{F}{J_M}, \quad f_1 = \frac{1}{L_e}, \quad f_3 = \frac{2}{3}\frac{p^2}{J_M}, \quad g_5 = \frac{p}{J_M},$$

and the other symbols are defined in Table 1.

Since our objective is that of designing an EKF that is able to estimate the whole system state starting from the measure of the stator currents, when speed varies slowly between two sample times, the mechanical equation can be neglected by putting the second member of (5) equal to zero. Moreover, with the aim of reducing the order of the model, the following complex state and input vectors are defined:

$$x = (x_1, x_2, x_3)^T = (i, \psi, \omega)^T = (i_\alpha + j i_\beta, \psi_\alpha + j\psi_\beta, \omega)^T,$$

and

$$u = u_\alpha + j u_\beta,$$

where j is the imaginary unit. In terms of the new complex state variables, choosing the complex current i as output and the complex stator voltage u as input, the dynamic model (1)–(5) becomes

$$\dot{x}_1 = -a_{11}x_1 + f_1(a_{22} - jx_3)x_2 + f_1 u, \tag{6}$$

$$\dot{x}_2 = a_{21}x_1 - (a_{22} - jx_3)x_2, \tag{7}$$

$$\dot{x}_3 = 0, \tag{8}$$

$$y = h(x) = x_1. \tag{9}$$

Table 1
Parameters of the induction motor model.

i_α (i_β)	Stator current component along α-axis (β-axis) fixed to the stator, A
u_α (u_β)	Stator voltage component along α-axis (β-axis), V
ψ_α (ψ_β)	Scaled rotor flux along α-axis (β-axis), Wb
ω	Rotor speed, el. rad/s
R_s (L_s)	Stator resistance (inductance), Ω (H)
L_m (L_r)	Mutual (rotor) inductance, H
R_r	Rotor resistance, Ω
τ_r	$\left(=\frac{L_r}{R_r}\right)$ rotor time constant, s
L_e	$\left(=L_s - \frac{L_m^2}{L_r}\right)$ stator equivalent inductance, H
F	Viscous friction coefficient, N m s
t_l	Load torque, N m
J_M	Inertia coefficient, N m s^2
p	Pole pairs
T_s	Sampling time, s
$\|\|\cdot\|\|$	Euclidean vector norm, corresponding to the induced norm for matrices
I_n	Identity matrix of order n

3. Observability conditions of the complex model

In this section the observability property of the dynamic model (6)–(9) is investigated. As is well known, the model in question is locally weakly observable if the observability matrix, of order $\infty \times n$, given by

$$O = \begin{pmatrix} dh(x) \\ dL_f h(x) \\ dL_f^2 h(x) \\ \vdots \end{pmatrix},$$

where $dh(x)$ is the gradient of h at x, $L_f h(x)$ is the Lie derivative of h along f, $L_f^k h(x) = L_f L_f^{k-1} h(x)$, and

$$f(x,u) = \begin{pmatrix} -a_{11}x_1 + f_1(a_{22} - jx_3)x_2 + f_1 u, \\ a_{21}x_1 - (a_{22} - jx_3)x_2, \\ 0 \end{pmatrix},$$

has rank equal to n.

That being stated, the following theorem gives necessary and sufficient conditions for the observability of the model (6)–(9).

Theorem 1. *Suppose that stator current measures, $y(t) = x_1(t)$ are available over an infinite time period $t \in [0, \infty)$. Then, the IM model*

(6)–(9) is locally weakly observable if, and only if

$$\psi^{(1)} \neq 0 \quad or \quad i^{(1)} \neq 0.$$

Moreover, if $u(t)$ is an analytical time-varying function, then the IM model is globally weakly observable, i.e. it is weakly observable at every initial states.

Proof. Observing that the model (6)–(9) is single-output, the Lie derivative $L_f^i h(x) = y^{(i)} = x_1^{(i)}$. It follows that matrix O can be obtained by computing the successive time-derivatives of x_1. Taking into account that $\dot{x}_3 = 0$, it is easy to verify that

$$y^{(1)} = x_1^{(1)} = -a_{11}x_1 + f_1(a_{22} - jx_3)x_2 + f_1 u, \tag{10}$$

and

$$y^{(i)} = x_1^{(i)} = -a_{11}x_1^{(i-1)} + f_1(a_{22} - jx_3)x_2^{(i-1)} + f_1 u^{(i-1)}, \tag{11}$$

for $i \geq 1$. Moreover, from (7) and (8), the following is obtained:

$$x_2^{(i)} = a_{21}x_1^{(i-1)} - (a_{22} - jx_3)x_2^{(i-1)}, \quad i = 2, 3, \ldots \tag{12}$$

Consider also the following gradients of x_1, $x_1^{(1)}$ and $x_1^{(2)}$:

$$dx_1 = \frac{\partial}{\partial x}x_1 = (1, 0, 0),$$

$$dx_1^{(1)} = \frac{\partial}{\partial x}x_1^{(1)} = (-a_{11}, f_1(a_{22} - jx_3), -jf_1 x_2),$$

$$dx_1^{(2)} = \frac{\partial}{\partial x}x_1^{(2)} = -a_{11}dx_1^{(1)} + f_1(a_{22} - jx_3)dx_2^{(1)} + (0, 0, -jf_1 x_2^{(1)}).$$

A first sufficient observability condition is obtained considering the following square matrix given by the first three rows of O:

$$O_1 = ((dx_1)^T, (dx_1^{(1)})^T, (dx_1^{(2)})^T)^T,$$

whose determinant

$$\det(O_1) = -jf_1^2(a_{22} - jx_3)x_2^{(1)} \tag{13}$$

vanishes only for $x_2^{(1)} = 0$, since the solution $x_3 = -ja_{22}$ is not admissible being the rotor speed variable x_3 a real number. The states corresponding to $x_2^{(1)} = 0$ are given by

$$\{x : x_2^{(1)} = 0\} = \{(x_1, a_{21}(a_{22} - jx_3)^{-1}x_1, x_3)^T\}. \tag{14}$$

In order to investigate on the model observability at the above states, one has to further proceed in the derivation of the system output function $h(x)$, computing the derivatives for $x_2^{(1)} = 0$. The gradient of the third temporal derivative of y, obtained from (11) for $i = 3$, is given by

$$dx_1^{(3)} = -a_{11}dx_1^{(2)} + f_1(a_{22} - jx_3)\, dx_2^{(2)} + (0, 0, -jf_1 x_2^{(2)}),$$

which, particularized for $x_2^{(1)} = 0$, becomes

$$dx_1^{(3)} = A(x)(-a_{11}, f_1(a_{22} - jx_3), -jf_1 x_2) + (0, 0, -jf_1 x_2^{(2)}),$$

where $A(x) = a_{11}^2 + f_1 a_{21}(a_{22} - jx_3)$. Since $x_2^{(2)} = a_{21}x_1^{(1)}$ for $x_2^{(1)} = 0$, the determinant of the matrix

$$O_2 = ((dx_1)^T, (dx_1^{(1)})^T, (dx_1^{(3)})^T)^T$$

results

$$\det(O_2) = -jf_1^2 a_{21}(a_{22} - jx_3)x_1^{(1)}. \tag{15}$$

Therefore, the matrix O_2 has full rank if, and only if, $x_1^{(1)} \neq 0$, which completes the sufficiency proof of the first part of the theorem, i.e. that the model (6)–(9) is locally weakly observable if $x_1^{(1)} \neq 0$ or $x_2^{(1)} \neq 0$. By inspection of (6) and (7), it is observed that $x_1^{(1)} = 0$ implies $x_2^{(1)} = 0$ and vice versa, $u(t)$ being constant. Consequently, the candidate unobservable states belong to the set Ω consisting of the states corresponding to $x_1^{(1)} = 0$ and $x_2^{(1)} = 0$, which can be parameterized by the rotor speed x_3 as follows:

$$\Omega = \{x : x_2^{(1)} = x_1^{(1)} = 0\} = \{(\overline{x}_1, \overline{x}_2(x_3), x_3)\}, \tag{16}$$

with

$$\overline{x}_1 = (a_{11} - a_{21}f_1)^{-1}(f_1 u),$$
$$\overline{x}_2(x_3) = (a_{22} - jx_3)^{-1}(a_{11} - a_{21}f_1)^{-1}(a_{21}f_1 u).$$

To prove the necessity, it needs to show that, starting from any two initial states $\overline{x}, \overline{x}^* \in \Omega$, with $\overline{x} = (\overline{x}_1, \overline{x}_2(\overline{x}_3), \overline{x}_3)^T$ and $\overline{x}^* = (\overline{x}_1, \overline{x}_2(\overline{x}_3^*), \overline{x}_3^*)^T$, the system displays the same output function, i.e.

$$y(t, \overline{x}, \overline{u}) = y(t, \overline{x}^*, \overline{u}), \quad \text{for all } t. \tag{17}$$

which means that Ω consists of unobservable states.

To this purpose, observe that the model in (6)–(9) can be solved in two steps as follows: first, the third equation is integrated and the following is obtained:

$$x_3(t) = x_{3,0}, \tag{18}$$

where $x_{3,0}$ is the initial rotor speed; by substituting (18) into the first two equations of the model, a linear dynamic system is obtained whose solution is given by

$$\begin{pmatrix} x_1(t) \\ x_2(t) \end{pmatrix} = e^{\tilde{A}(x_{3,0})t}\left(\begin{pmatrix} x_{1,0} \\ x_{2,0} \end{pmatrix} + \int_0^t e^{-\tilde{A}(x_{3,0})\tau}\tilde{B}u(\tau)\, d\tau\right),$$

where $x_{1,0}$ and $x_{2,0}$ are two initial states and

$$\tilde{A}(x_{3,0}) = \begin{pmatrix} -a_{11} & f_1(a_{22} - jx_{3,0}) \\ a_{21} & -(a_{22} - jx_{3,0}) \end{pmatrix}, \quad \tilde{B} = \begin{pmatrix} f_1 \\ 0 \end{pmatrix}.$$

Based on this, (17) can be rewritten as follows:

$$y(t, \overline{x}, \overline{u}) - y(t, \overline{x}^*, \overline{u}) = \tilde{C}(e^{\tilde{A}(\overline{x}_3)t}\overline{x} - e^{\tilde{A}(\overline{x}_3^*)t}\overline{x}^*) + \tilde{C}\int_0^t (e^{\tilde{A}(\overline{x}_3)(t-\tau)} - e^{\tilde{A}(\overline{x}_3^*)(t-\tau)})\tilde{B}u(\tau)\, d\tau, \tag{19}$$

for all t, where $\tilde{C} = (1, 0)$. From (19), a necessary and sufficient condition for (17) to hold is that the time derivatives of order $i = 0, 1, \ldots$ of the condition itself are all simultaneously null, at any arbitrary fixed instant. The derivatives of order $i=0$ and $i=1$, evaluated at $t=0$, give the conditions

$$\overline{x}_1 - \overline{x}_1^* = 0,$$
$$-a_{11}(\overline{x}_1 - \overline{x}_1^*) + f_1((a_{22} - j\overline{x}_3)\overline{x}_2(\overline{x}_3) + (a_{22} - j\overline{x}_3^*)\overline{x}_2(\overline{x}_3^*)) = 0,$$

that are satisfied by all, and only, the points in Ω. Moreover, recall that, whenever two functions $\phi(t)$ and $\gamma(t)$ have the same derivatives of order k w.r.t. the independent variable t, the successive derivatives must also be the same. This can be proved by recursive application of the relation

$$\phi^{(k+1)}(t) = \frac{d}{dt}\phi^{(k)}(t) = \frac{d}{dt}\gamma^{(k)}(t) = \gamma^{(k+1)}(t).$$

By choosing $\phi(t) = y(t, \overline{x}, \overline{u}) - y(t, \overline{x}^*, \overline{u})$ and $\gamma(t) = 0$, and observing that the two functions have equal derivatives of order $i=1$, it can be concluded that the successive derivatives introduce no further indistinguishability constraints, and thus every pair of points $\overline{x}$ and $\overline{x}^*$ in Ω is indistinguishable. This also proves the necessity of the observability condition stated in the first part of the theorem. In fact, assuming by contradiction that the model (6)–(9) is weakly observable and the conditions $\psi^{(1)} \neq 0$ or $i^{(1)} \neq 0$ are not satisfied, i.e. $\psi^{(1)} = 0$ or $i^{(1)} = 0$, the model displays a set of states, Ω, containing indistinguishable states, which is in contrast with the hypothesis of observability.

Let us now move on to the second part of the theorem. The fourth temporal derivative of the system output is obtained from (11) for $i=4$, and the corresponding gradient is given by

$$dx_1^{(4)} = -a_{11}\, dx_1^{(3)} + f_1(a_{22} - jx_3)\, dx_2^{(3)} + B(x)$$
$$= [-a_{11} + a_{21}f_1(a_{22} - jx_3)]\, dx_1^{(3)} + B(x)$$

with $B(x)=(0,0,-jf_1x_2^{(3)})$. This gradient, particularized for $x_1^{(1)}=0$ and $x_2^{(1)}=0$, becomes

$$dx_1^{(4)} = -a_{11}(0,f_1(a_{22}-jx_3),-jf_1x_2) + f_1(a_{22}-jx_3)(0,f_1(a_{22}-jx_3),-jf_1x_2)+(0,0,-jf_1x_2^{(3)}).$$

Then, it is possible to compute the following matrix O_3, given by

$$O_3=((dx_1)^T,(dx_1^{(1)})^T,(dx_1^{(4)})^T)^T,$$

whose determinant, particularized for $x_1^{(1)}=0$ and $x_2^{(1)}=0$, is given by

$$\det(O_3)=-jf_1^3(a_{22}-jx_3)a_{21}u^{(1)}, \tag{20}$$

which can only vanish for $u^{(1)}=0$. Furthermore, the determinant of the generic observability matrix O_k, constructed with the gradient of the kth output function derivative, i.e.

$$O_k=((dx_1)^T,(dx_1^{(1)})^T,(dx_1^{(k)})^T)^T,$$

can only vanish if $u^{(k)}=0$. This completes the proof of the theorem because it shows that, for any analytic time-varying input function $u(t)$, there exists at least one determinant that is not null. □

Remark 1. Comparing these results with the literature, it is useful to underline that the most employed criterion for assessing observability property for nonlinear systems is the rank condition, defined on a $\infty\times n$ matrix, which gives sufficient conditions (Canudas De Wit et al., 2000; Hermann & Krener, 1977; Marino et al., 2010; Reif et al., 1999). In Canudas De Wit et al. (2000), the rank condition is used for obtaining also necessary conditions considering a sixth order EKF which includes the mechanical equation and defines an augmented state vector including the torque as the sixth state variable. In this paper, instead, the rank condition is used as a sufficient condition for observability, as it is claimed in the literature, and we introduce new arguments of analysis for obtaining necessary conditions for the fifth order EKF. These arguments regard the determination of the states of the fifth order model of the system at constant speed which are candidate to be unobservable, and the successive testing that these states are effectively observable, providing that the input $u(t)$ is time-varying and continuously differentiable. Moreover, the observability property is verified considering the discrete-time model of the above fifth order system, which is the correct property to be verified, taking into account that the model is used for designing a discrete-time EKF.

4. Observability of the discrete-time model

In this section it is shown that the observability propriety of the IM is preserved by a time discretization. By applying the first-order Euler approximation to the continuous-time dynamics in (6)–(9), the following discrete-time IM model can be obtained

$$\begin{aligned} x_1(k+1)&=\tilde a_{11}x_1(k)+\tilde f_1(a_{22}-jx_3(k))x_2(k)+\tilde f_1u(k),\\ x_2(k+1)&=\tilde a_{21}x_1(k)+(1-T_s(a_{22}-jx_3(k)))x_2(k),\\ x_3(k+1)&=x_3(k), \end{aligned} \tag{21}$$

where $\tilde a_{11}=1-a_{11}T_s$, $\tilde f_1=f_1T_s$, $\tilde a_{21}=a_{21}T_s$, with system output given by

$$y(k)=h(x(k))=x_1(k).$$

Let us denote with $x(k+1)=\tilde g(x(k))$ the above dynamic model in (21). The first row of the observability matrix O is given by

$$dh_1=\left.\frac{\partial h(x)}{\partial x}\right|_{x(k)}=(1\quad 0\quad 0),$$

which is independent of the value of $x(k)$. The Jacobian matrix of $\tilde g$ at $x(k)$ is given by

$$\left.\frac{\partial\tilde g(x)}{\partial x}\right|_{x(k)}=\begin{pmatrix}\tilde a_{11} & \tilde f_1(a_{22}-jx_3(k)) & -j\tilde f_1x_2(k)\\ \tilde a_{21} & 1-T_s(a_{22}-jx_3(k)) & jT_sx_2(k)\\ 0 & 0 & 1\end{pmatrix}. \tag{22}$$

The second row of the observability matrix O is given by

$$\begin{aligned} dh_2&=\left.\frac{\partial h(x)}{\partial x}\right|_{x(k+1)}\left.\frac{\partial\tilde f(x)}{\partial x}\right|_{x(k)}\\ &=(\tilde a_{11}\quad \tilde f_1(a_{22}-jx_3(k))\quad -j\tilde f_1x_2(k)). \end{aligned}$$

The Jacobian matrix of $\tilde g$ at $x(k+1)$ can be easily obtained from (22) by replacing $x(k)$ with $x(k+1)$. Thus, the third row of the observability matrix O is given by

$$\begin{aligned} dh_3&=\left.\frac{\partial h(x)}{\partial x}\right|_{x(k+2)}\left.\frac{\partial\tilde g(x)}{\partial x}\right|_{x(k+1)}\left.\frac{\partial\tilde g(x)}{\partial x}\right|_{x(k)}\\ &=(\tilde a_{11}\quad \tilde f_1\eta(k+1)\quad -j\tilde f_1x_2(k+1))\left.\frac{\partial\tilde g(x)}{\partial x}\right|_{x(k)}\\ &=(A\quad B\quad C), \end{aligned}$$

where $\eta(k)=a_{22}-jx_3(k)$, A is a term whose expression can be omitted, since it does not affect the value of the observability matrix determinant, whilst B and C are given by

$$\begin{aligned} B&=\tilde f_1(\tilde a_{11}\eta(k)+(1-T_s\eta(k))\eta(k+1)),\\ C&=j\tilde f_1(\eta(k+1)T_sx_2(k)-x_2(k+1)-\tilde a_{11}x_2(k)). \end{aligned}$$

Finally, by exploiting the third equation of the dynamics model, $x_3(k+1)=x_3(k)$, it is possible to find, by direct computation, that the determinant of the observability matrix O is given by

$$\det(O)=j\tilde f_1^2\eta(k)(x_2(k)-x_2(k+1)),$$

which can only vanish for constant rotor flux, i.e. $x_2(k+1)=x_2(k)$. Hence, the discrete-time model in (21) is locally weakly observable if the rotor flux is not constant, i.e. $x_2(k+1)\neq x_2(k)$.

5. Filter derivation

To obtain an estimate of the complex-valued state x of the nonlinear model (6)–(9), an extended complex Kalman filter has to be considered (Petersen & Savkin, 1999). The filter has the same structure of a standard real EKF, except for the fact that the covariance matrix of the estimation error is Hermitian, i.e. $P_k=P_k^H$, and the dynamical matrix of the underlying linearized model has complex-valued entries.

As a first step, a stochastic discrete-time model of the IM is obtained by applying Euler's approximation method to the (6)–(9). This yields

$$\begin{cases} x_{k+1}=g_k(x_k,u_k)+w_k,\\ y_k=h_k+v_k, \end{cases} \tag{23}$$

where $x_k=(x_{1,k},x_{2,k},x_{3,k})^T$, w_k and v_k are white Gaussian noise processes with covariance matrices given by Q_k and R_k, respectively, and

$$h_k=x_{1,k},$$

$$g_k=\begin{pmatrix}\tilde a_{11}x_{1,k}+\tilde f_1(a_{22}-jx_{3,k})x_{2,k}+\tilde f_1u_k\\ \tilde a_{21}x_{1,k}+(1-T_sa_{22}+jT_sx_{3,k})x_{2,k}\\ x_{3,k}\end{pmatrix}.$$

The processes w_k and v_k are assumed to be uncorrelated between them and w.r.t. the system state variables.

The ECKF is described by the following recursive algorithm involving, as usual, *time update* and a *measurement update* phases. During the kth time update phase, a priori estimates of the system state and of the error covariance matrix are computed as follows:

$$\hat{x}_{k+1|k} = g_k(\hat{x}_{k|k}, u_k), \tag{24}$$

$$P_{k+1|k} = F_k P_{k|k} F_k^H + Q_k, \tag{25}$$

where F_k is the dynamic matrix of the linearized model and is given by

$$F_k = \left.\frac{\partial g_k(x_k)}{\partial x}\right|_{x=\hat{x}_{k|k}} = \begin{pmatrix} \tilde{a}_{11} & \tilde{f}_1(a_{22} - jx_{3,k|k}) & -j\tilde{f}_1 x_{2,k|k} \\ \tilde{a}_{21} & 1 - a_{22}T_s + jT_s x_{3,k|k} & jT_s x_{2,k|k} \\ 0 & 0 & 1 \end{pmatrix}.$$

During the kth measurement update phase, a posteriori estimates are computed as follows:

$$\hat{x}_{k|k} = \hat{x}_{k|k-1} + L_k(y_k - H_k\hat{x}_{k|k-1}), \tag{26}$$

$$P_{k|k} = P_{k|k-1} - L_k H_k P_{k|k-1}, \tag{27}$$

where

$$L_k = P_{k|k-1}H_k^T(H_k P_{k|k-1} H_k^T + R_k)^{-1}, \tag{28}$$

and H_k is the output matrix of the linearized model and is given by

$$H_k = \left.\frac{\partial h(x_k)}{\partial x}\right|_{x=\hat{x}_{k|k}} = [1\ \ 0\ \ 0].$$

The filter is initialized, at the instant $k=0$, with $\hat{x}_{0|0} = 0$ and $P_{0|0} = P_0$, where $P_0 \in \mathbb{R}^{3\times 3}$ represents the initial estimate error covariance.

Remark 2. It is worth noting that the following facts are the rational reasons for the processing time reduction:

1. The reduction of the order of the filter lead to a reduction of the number of operations as shown in Grewal and Andrews (2011, Table 7.2), where the presented formulas demonstrate that the number of operations increases with the order of all the involved matrices.
2. No matrix inversion is required in the proposed ECKF, indeed in (28) the term $(H_k P_{k|k-1} H_k^T + R_k)$ is a scalar (instead it is a matrix in the 5th order EKF), moreover this scalar is also real because H and R contain real elements and it is easy to see that P matrix contains only real elements. So the operation of matrix inversion that is necessary in the classic 5th order EKF is translated in the inverse of a real number in the proposed ECKF.
3. In the standard real-valued implementation the complexity of the model can be reduced taking into consideration that many elements of matrix H are zeros and manipulating the relations of the filter (Hilairet, Auger, & Darengosse, 2000). This fact is automatically included in the present complex formulation.
4. Matrices Q, R, $P_{k|k}$, $P_{k|k-1}$, L_k have real elements also in the complex form of the EKF, while their order is 3 instead of 5, as in the standard real-valued implementation.

It is worth noting that in the literature the problem of reducing the time of complexity of the estimation process has been dealt with by some authors, such as Hilairet, Auger, and Berthelot (2009, 2000). More precisely, Hilairet et al. (2000) proposed a more efficient filtering process which exploits the structural form of the IM model, while Hilairet et al. (2009) obtained an improvement of 25% by deriving a two-stage EKF that is based on the procedure described in Hsieh and Chen (1999) and Hsieh (2003) and that uses suitable transformation matrices.

6. Simulation results

The proposed ECKF estimator has been evaluated by means of simulations that have been carried out in the Matlab/Simulink environment. The Simulink model includes the real-valued IM model (1)–(5), the ECKF estimator (24)–(28), and the controller. As for the IM model, the following nominal parameters have been used that have been estimated according to the procedure described by Alonge, D'ippolito, and Raimondi (2001) and that are related to a real 0.75-kW IM:

$$R_s = 15.6808\ \Omega, \quad L_s = 0.5236\ \text{H}, \quad L_e = 4.30 \times 10^{-2}\ \text{H},$$
$$\tau_r = 6.69 \times 10^{-2}\ \text{s}, \quad p = 2, \quad J_m = 5.6 \times 10^{-3}\ \text{N m s}^2,$$
$$F = 2.3 \times 10^{-3}\ \text{N m s}.$$

A field oriented vector controller, such as that described by e.g. Vas (1998) and Leonhard (2001), has been realized, which involves four PI sub-controllers that have been designed as described by Alonge, D'Ippolito, Raimondi, and Urso (2001). The flux and speed loops have been closed by means of the proposed ECKF providing a full estimation of the IM's state. A frequency of 10 kHz has been adopted for the execution of both the controller and the ECKF.

As is well known, the tuning of the values of the covariance matrices Q and R is still an open problem. In the majority of the papers in the literature the values of the matrices Q and R are preassigned or computed based on a trial-and-error procedure. This is the reason why in different papers different values are proposed for the two matrices although they are determined for the same prototype. Hilairet et al. (2000, 2009) provided a rule based on the minimization of the mean square error between the estimated variables and the actual ones. Our approach has been that of fixing the covariance matrix $R=1$ and then determining the covariance matrix Q by the trial-and-error method. This approach is theoretically justified by the known fact that only the ratios between the elements of Q and R affect the system behavior (Bittanti & Savaresi, 2000). By doing this we have determined $Q = \text{diag}(1, 10^{-3}, 10)$.

6.1. Robustness analysis

In the following a robustness analysis of the proposed ECKF is carried out, by evaluating its ability to produce accurate state estimates also when the model parameters are varied. A similar study is carried out by Alonge and D'Ippolito (2007) for a reduced-order rotor flux optimal observer. The ECKF has been implemented with detuned parameters, while the IM model contains nominal parameters.

A first study is carried out by analyzing the behavior of the ECKF when the IM is operated at rated rotor speed and rated load. Fig. 1 shows the steady-state estimation errors when the mutual inductance L_m, the rotor resistance R_r, and the rotor resistance R_s are varied. More precisely, Fig. 1a–c shows the flux estimation error as mutual inductance is increased up to 50% of its nominal value, the rotor resistance up to 300%, and stator resistance up to 50%, respectively (in the figures the modified values are indicated by the subscript m'). Fig. 1d–f reports results of the same analysis as for what it concerns the rotor speed estimation error. As it can be seen, the influence of these parameters' variations is small, which shows a good robustness of the ECKF. A different behavior can be observed when the machine operates at low speed (Fig. 2), when a small variation of the stator resistance produces a high error in the flux and speed estimates (cf. Fig. 2c and f). Moreover, it is worth noting that Fig. 1a also reveals that a variation of L_m up to 50% of its nominal value can produce a high flux estimation error of 40%, even at rated, low rotor speed.

From this analysis it is clear that the more critical condition is a variation of the stator resistance when the machine is operated at low speed. Therefore, it is of particularly important an accurate R_s estimation which, normally, is not a problem, because it could be measured directly. Obviously the main source of variation is temperature, so in practical application R_s can be scheduled depending on motor temperature, but it is not trivial.

As for what it concerns the sensitivity of the ECKF to noisy measurement, Table 2 reports the mean and the standard deviations of the rotor speed and of the flux estimation errors, in the absence of noise and when a white noise is superimposed to the measured signal. As it can be seen the ECKF is robust to noise, since both the means and the standard deviations of the estimation errors remain limited and small also in the presence of noise.

6.2. Closed loop simulation results

In order to assess the behavior of the closed loop system, consisting of the IM model, a PI-based controller, and the ECKF, we have carried out the following simulation. At the beginning of the simulation a null reference signal is specified for the rotor speed and a step signal with an amplitude of 1 Wb is specified as the rotor flux reference. After 1 s, a step signal with an amplitude of 100 rad/s is specified as the rotor speed reference, while after other 2 s a step signal of 3 N m is applied as the input load torque. Figs. 3–6 summarize the most significant results of the simulation, which we can now comment in view of Theorem 1. By focusing on Figs. 3 and 6 it is possible to see that, when the IM is fluxed at a zero reference speed, the stator current components and the rotor flux become constant, after a short transient, as well as the two stator voltages. In this initial instant, the observability conditions of Theorem 1 are not satisfied, but the ECKF is still able to correctly estimate the rotor speed since also the load torque is null. In the presence of a non-null input load torque signal, as long as the rotor speed signal is also not null, the observability conditions of Theorem 1 are met and the ECKF can correctly estimate the system state (cf. the figures during the interval [3, 5]). As soon as the rotor speed approaches zero and an active load torque is applied while the IM is still fluxed, the observability conditions of Theorem 1 are not satisfied. Under these conditions the ECKF is unable to correctly estimate the system state. Indeed the model (1)–(5) works at constant current, without motor torque production, therefore the speed becomes negative and converges to a value such that the load torque matches the viscous friction torque, whereas ECKF always gives a speed equal to zero. It is worth noticing that this operating condition is critical for every model-based estimator or observer.

7. Experimental results

In this section experimental results are presented validating the proposed 5th order ECKF on the experimental viewpoint. To this purpose, a closed loop control system has been realized that is composed of the above IM, supplied by a voltage source inverter, a powder brake which applies the load t_l to the motor, a four-loop PI-type controller, already described in Section 6, and the proposed ECKF which computes online state estimates that are used by the controller. The IM has been operated with a rotor flux of 1 Wb. Both the controller and the estimator ECKF have been implemented on a platform involving a dSPACE 1103 microcontroller, operating under the Matlab/Simulink environment. The use of the dSPACE platform is particularly important since it allows rapid prototyping of the control system and a real-time execution of it. The covariance matrices Q_k and R_k have been assumed to be constant and equal to $Q = \mathrm{diag}(1, 10^{-3}, 10)$ and $R = 1$ (as in simulation tests). The IM has been fluxed during the first 0.5 s, and the stator currents have been measured by using two Hall-effect transducers.

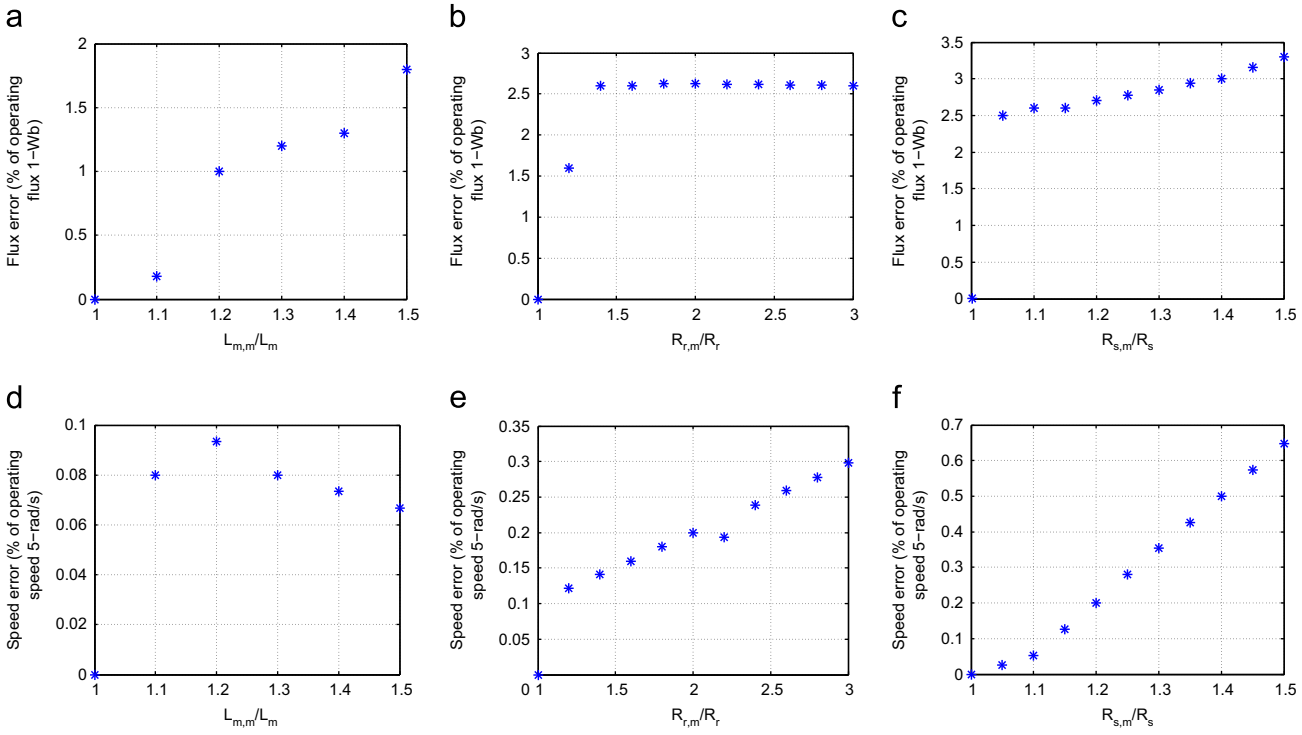

Fig. 1. Simulation results at rated rotor speed (150 rad/s) and rated load, showing robustness performance of the proposed ECKF estimator: (a) flux error vs. L_m variation, (b) flux error vs. R_r variation, (c) flux error vs. R_s variation, (d) speed error vs. L_m variation, (e) speed error vs. R_r variation, and (f) speed error vs. R_s variation.

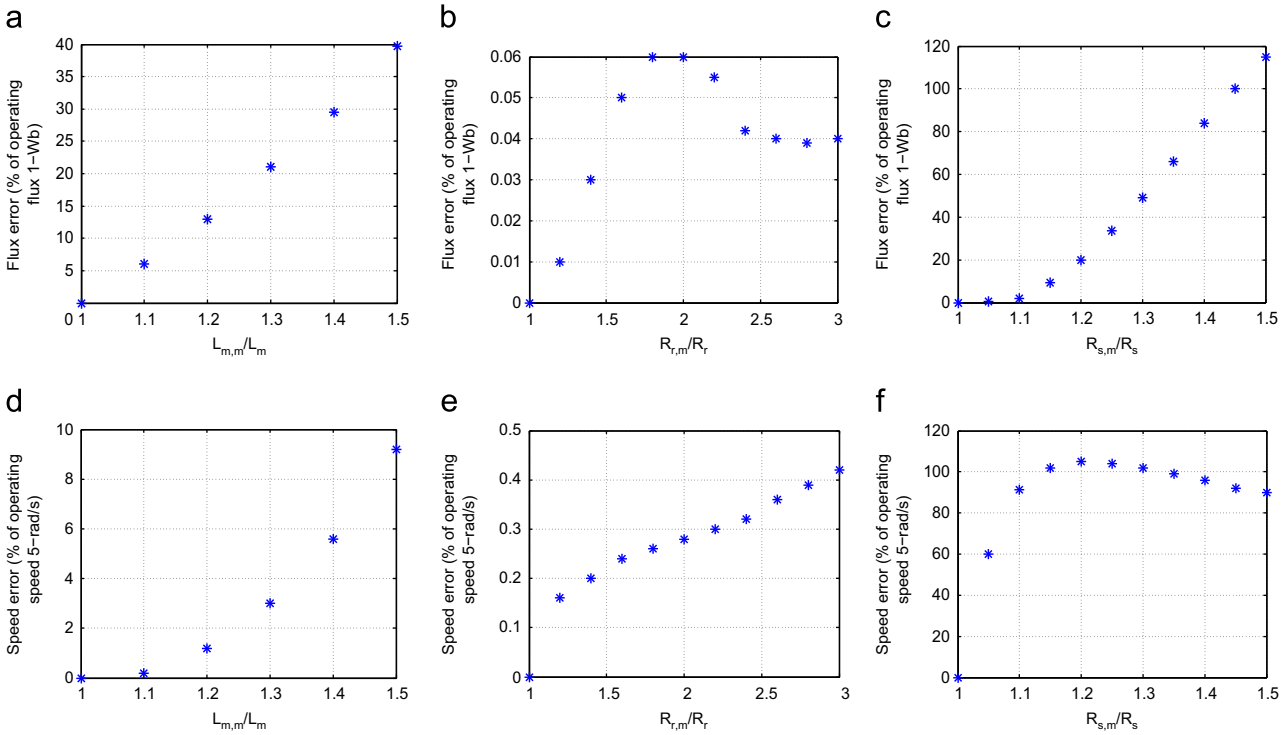

Fig. 2. Simulation results at low rotor speed (5 rad/s) and rated load, showing robustness performance of the proposed ECKF estimator: (a) flux error vs. L_m variation, (b) flux error vs. R_r variation, (c) flux error vs. R_s variation, (d) speed error vs. L_m variation, (e) speed error vs. R_r variation, and (f) speed error vs. R_s variation.

Table 2
Noise sensitivity of ECKF.

Type of test	No noisy measures	Noisy measures
Test at 150 rad/s		
Standard deviation of the speed (rad/s)	0.05	0.7
Standard deviation of the flux estimate (Wb)	0.04	0.05
Mean error of the speed estimate (%)	0	0
Mean error of the flux estimate (%)	0	0
Test at 5 rad/s		
Standard deviation of the speed (rad/s)	0.06	0.5
Standard deviation of the flux estimate (Wb)	0.02	0.04
Mean error of the speed estimate (%)	0	0
Mean error of the flux estimate (%)	0	0

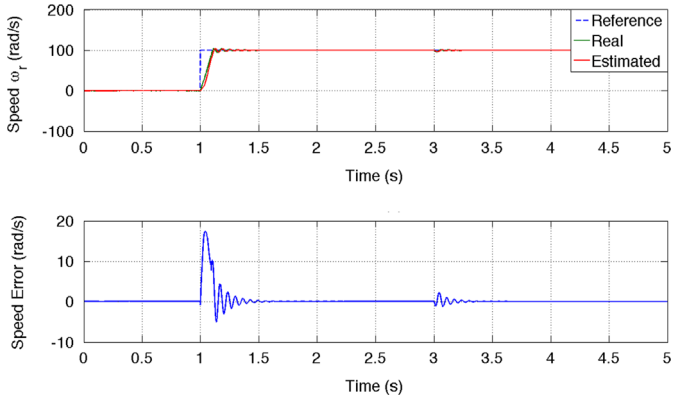

Fig. 3. Rotor speed $x_{3,k}$ and estimation error $e_{3,k}=\omega_{r,k}-\hat{\omega}_{r,k}$ applying a speed step of 100 rad/s and a load torque, with feedback from ECKF.

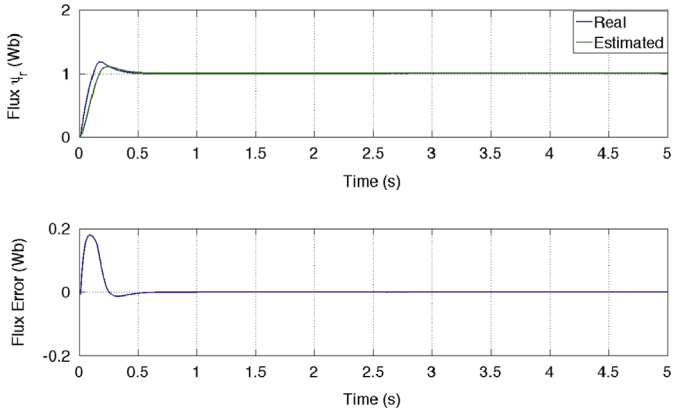

Fig. 4. Norm of the rotor flux, $|x_{2,k}|$, and of the flux estimation error, $e_{2,k}=|x_{2,k}|-|\hat{x}_{2,k}|$, applying a speed step of 100 rad/s and a load torque, with feedback from ECKF.

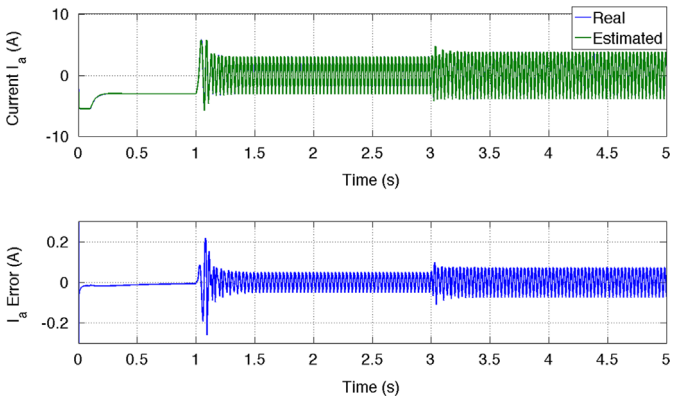

Fig. 5. Stator current and stator estimation error (defined as $e_{\Re(x_{1,k})}=\Re(x_{1,k})-\Re(\hat{x}_{1,k})$) along the α-axis ($\Re(x_{1,k})$ and $\Re(e_{1,k})$, respectively), applying a speed step of 100 rad/s and a load torque, with feedback from ECKF.

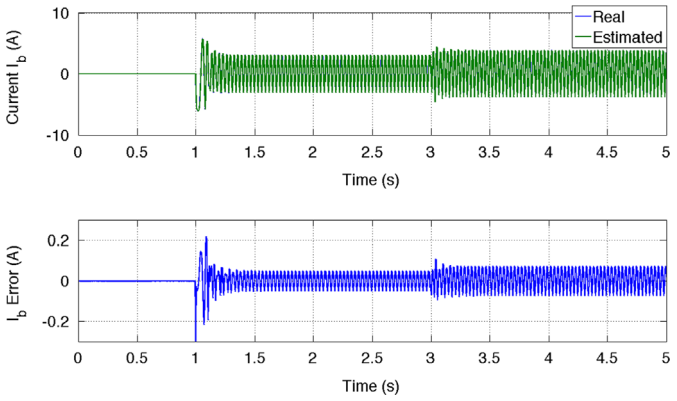

Fig. 6. Stator current and stator estimation error (defined as $e_{\Im(x_{1,k})}=\Im(x_{1,k})-\Im(\hat{x}_{1,k})$) along the β-axis ($\Im(x_{1,k})$ and $\Im(e_{1,k})$, respectively), applying a speed step of 100 rad/s and a load torque, with feedback from ECKF.

Two experiments have been performed, one at high rotor speed and with load (see Fig. 7), and one at low rotor speed (Fig. 8). The behavior of the system at high speed is satisfactory as discussed in the following. The rotor speed correctly tracks the reference one, with relatively high error only during a first transient (cf. Fig. 7e and f), and reaches the steady-state operations without final error. In the presence of the load torque signal shown in Fig. 7d, whose value is 3 N m, the speed tracking error is negligible. By applying a descended ramp reference speed, when the speed approaches zero, the tracking error initially increases up to 4 rad/s, but rapidly converges afterward to zero. During steady-state operation at -150 rad/s, the load torque is removed (at $t=13$ s) without speed error, whereas a speed error of about 9 rad/s occurs when the reference speed increases to lead the motor at the standstill. The rotor flux reaches a value of 1 Wb and remains almost constant during the entire duration of the experiments, except for operations at zero reference speed, when the rotor flux varies from 0.92 to 1.08. The stator currents are under the maximum allowed values during all the operating conditions. Note that, since the load torque is measured by a sensor that is inserted into the brake, the oscillations that are present in it are not caused by the controller or the estimator designed for the experiments, but rather from the load itself. At low rotor speed the behavior of the system is also satisfactory up to a reference speed of 5 rad/s (see Fig. 8e). At 2 rad/s rotor speed a transient oscillation of the tracking error occurs, where a slow convergence to the steady state can be observed. The estimation of the rotor flux appears accurate during all the operating conditions. This fact can also be verified indirectly, by observing that the closed-loop system nicely behaves during all the above operating conditions.

A second experiment has been performed with the aim of analyzing the behavior of the real system w.r.t. observability conditions of Theorem 1. The experiment starts by giving zero reference signal for the rotor speed and 1-Wb signal for the rotor flux reference in order to flux the IM. At the instant $t=1$ s a 15-rad/s reference signal is applied for the rotor speed, and at the instant

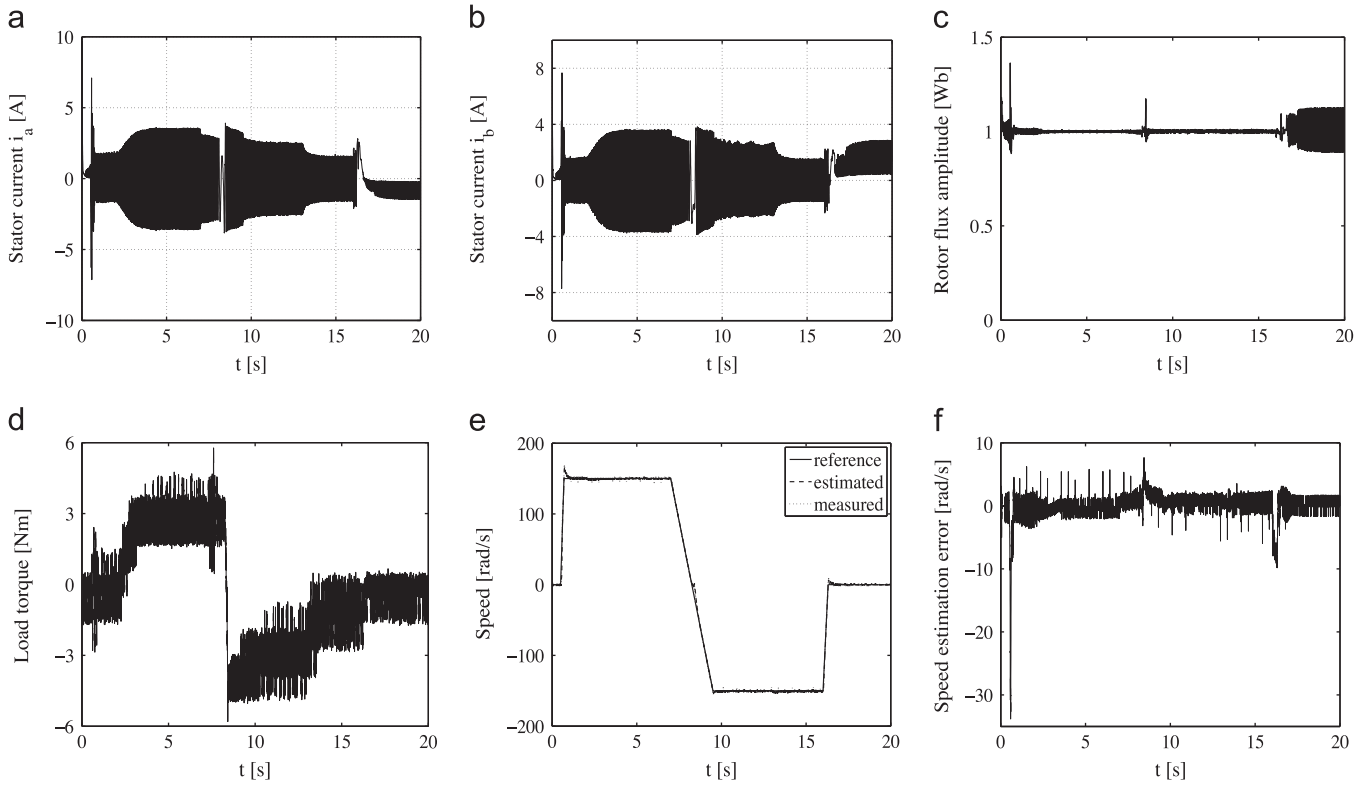

Fig. 7. Experimental results at high rotor speed: (a) stator current along α-axis in fixed frame, (b) stator current along β-axis in fixed frame, (c) amplitude of the rotor flux vector, (d) applied load torque, (e) reference, estimated and actual speed, and (f) speed estimation error $e_\omega=\omega_{r,k}-\hat{\omega}_{r,k}$.

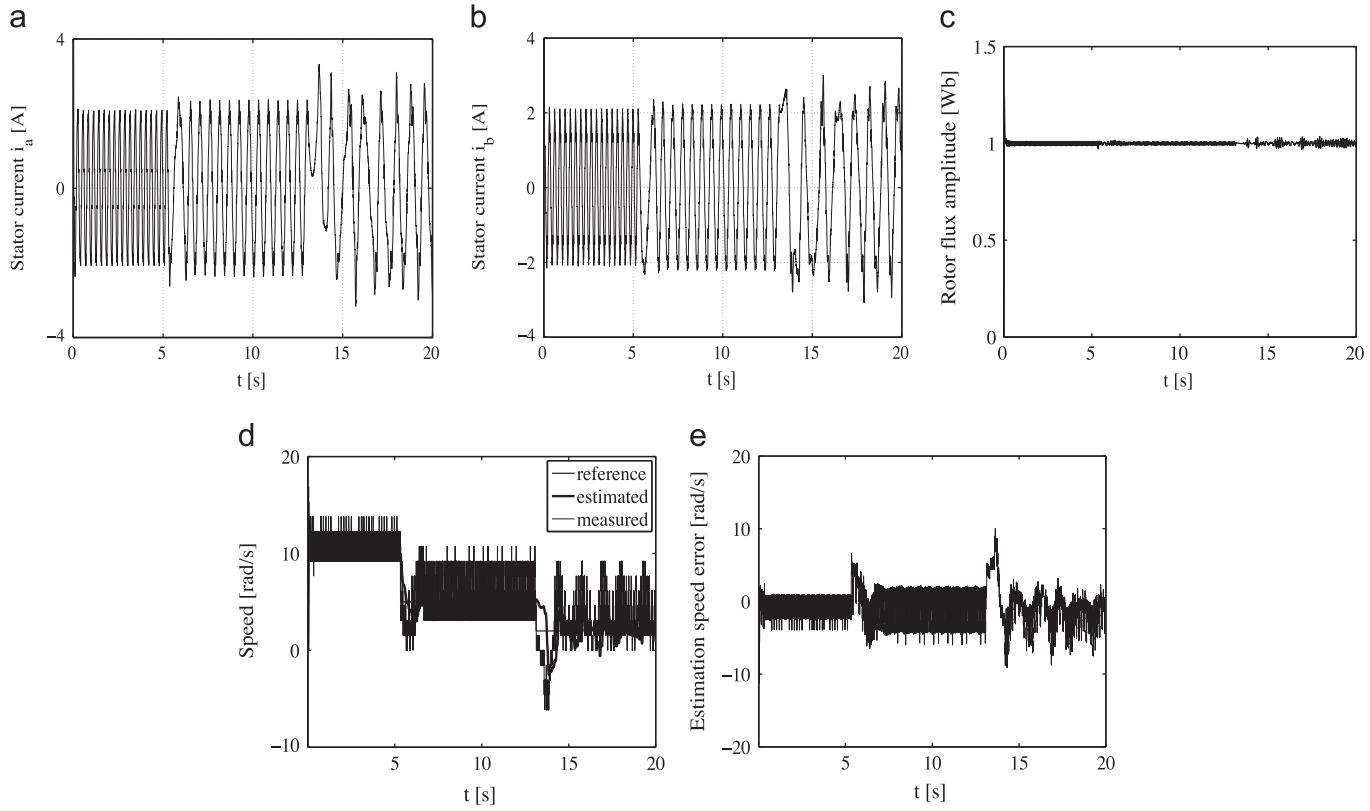

Fig. 8. Experimental results at low rotor speed: (a) stator current along α-axis in fixed frame, (b) stator current along β-axis in fixed frame, (c) amplitude of the rotor flux vector, (d) reference, estimated and actual speed, and (e) speed estimation error $e_\omega = \omega_{r,k} - \hat{\omega}_{r,k}$.

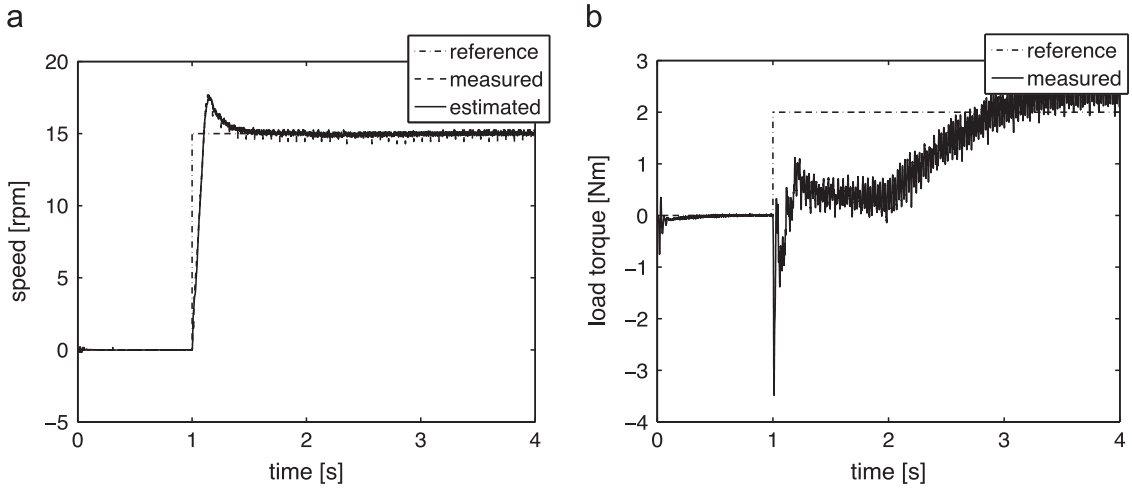

Fig. 9. Experimental results at low rotor speed and load: (a) reference, estimated and measured speed and (b) applied load torque.

$t=2$ s a load torque command of 2 N m is applied to the motor by using the powder brake. Fig. 9 reports the result of this experiment and shows that an accurate estimation of the rotor speed is obtained, also when the IM operates at low speed and with load torque. Furthermore, Fig. 8d and e shows that, when the rotor speed decreases down to 2 rad/s, the speed estimate degrades as it can be expected by the fact that the IM is operating in the neighborhood of the region where the observability conditions are not met. A similar behavior can be observed when the rotor speed reference signal is reversed from a positive to a negative value. As the real rotor speed approaches zero, the speed estimation error increases, but then it converges again to zero when the IM leaves the region where the observability conditions are not met (Fig. 7e and f). Finally, at zero reference speed, the filter gives the correct speed only at zero load torque (see last time interval in Fig. 7e).

It should be finally said that the complex-valued model of the IM describes exactly the same behavior of the more traditional 5th order model. Therefore, the proposed ECKF produces exactly the same results of the corresponding more traditional EKF, generated based on the 5th order IM model under the hypothesis of constant speed, i.e. $\dot{\omega} = 0$. While it is already apparent that the complex-valued model allows an easier and more compact observability analysis, its advantage also concerns the fact that the ECKF requires lower computational effort, as discussed in Remark 2.

Processing of both the proposed ECKF and the conventional 5th order EKF, the latter being shaped by using Simulink blocks and an ad hoc 2×2 inversion algorithm, shows that a 35% reduction time is obtained with the ECKF.

8. Conclusion

In this work necessary and sufficient conditions for the local weak observability of a complex-valued model of the IM were provided. An ECKF has been designed to estimate the state of the IM during different operating conditions, whose estimation property was evaluated through simulations in the Matlab–Simulink environment. The effectiveness of the ECKF was also tested by employing a dSPACE micro-controller on an experimental testbed. Results showed that, as long as the observability conditions of Theorem 1 are met, the ECKF is able to provide accurate state estimates, with or without a load torque. It is worth noticing that the ECKF can correctly operate even with low rotor speed ($\omega \to 0$), as long as the input stator voltage is varying. Moreover, the implementation of the complex-valued state estimator was shown to be advantageous over the standard real-valued filter, in terms of a 35% reduction of the required computation time.

References

Alonge, F., & D'Ippolito, F. (2007). Design and sensitivity analysis of a reduced-order rotor flux optimal observer for induction motor control. *Control Engineering Practice*, *15*(12), 1508–1519.

Alonge, F., & D'Ippolito, F. (2010). Extended Kalman filter for sensorless control of induction motors. In *First symposium on sensorless control for electrical drives* (SLED) (pp. 107–113).

Alonge, F., D'ippolito, F., & Raimondi, F. (2001). Least squares and genetic algorithms for parameter identification of induction motors. *Control Engineering Practice*, *9*(6), 647–657.

Alonge, F., D'Ippolito, F., Raimondi, F., & Urso, A. (2001). Method for designing pi-type fuzzy controllers for induction motor drives. *IEE Proceedings—Control Theory and Applications*, *148*(1), 61–69.

Alonge, F., D'Ippolito, F., & Sferlazza, A. (2014). Sensorless control of induction motor drive based on robust Kalman filter and adaptive speed estimation. *IEEE Transactions on Industrial Electronics*, *61*(3), 1444–1453.

Bittanti, S., & Savaresi, S. M. (2000). On the parametrization and design of an extended Kalman filter frequency tracker. *IEEE Transactions on Automatic Control*, *45*(9), 1718–1724.

Buyamin, S. (July 2007). *Optimization of the extended Kalman filter for speed estimation of induction motor drives* (Ph.D. thesis). UK: School of Electrical, Electronic and Computer Engineering, Newcastle University.

Canudas De Wit, C., Youssef, A., Barbot, J., Martin, P., & Malrait, F. (2000). Observability conditions of induction motors at low frequencies. In *IEEE conference on decision and control* (Vol. 3, pp. 2044–2049). ⟨http://dx.doi.org/10.1109/CDC.2000.914093⟩.

Cirrincione, M., Pucci, M., Cirrincione, G., & Capolino, G.-A. (2004). A new TLS-based MRAS speed estimation with adaptive integration for high-performance induction machine drives. *IEEE Transactions on Industry Applications*, *40*(4), 1116–1137.

Cirrincione, M., Pucci, M., Cirrincione, G., & Capolino, G.-A. (2006). An adaptive speed observer based on a new total least-squares neuron for induction machine drives. *IEEE Transactions on Industry Applications*, *42*(1), 89–104.

Ghanes, M., De Leon, J., & Glumineau, A. (2006). Observability study and observer-based interconnected form for sensorless induction motor. In *45th IEEE conference on decision and control* (pp. 1240–1245). IEEE.

Ghanes, M., & Zheng, G. (2009). On sensorless induction motor drives: *Sliding-mode observer and output feedback controller*. *IEEE Transactions on Industrial Electronics*, *56*(9), 3404–3413.

Grewal, M. S., & Andrews, A. P. (2011). *Kalman filtering: Theory and practice using MATLAB*. Wiley.com.

Hermann, R., & Krener, A. (1977). Nonlinear controllability and observability. *IEEE Transactions on Automatic Control*, *22*(5), 728–740.

Hilairet, M., Auger, F., & Berthelot, E. (2009). Speed and rotor flux estimation of induction machines using a two-stage extended Kalman filter. *Automatica*, *45*(8), 1819–1827.

Hilairet, M., Auger, F., & Darengosse, C. (2000). Two efficient Kalman filters for flux and velocity estimation of induction motors. In *2000 IEEE 31st annual power electronics specialists conference, PESC* (Vol. 2, pp. 891–896). IEEE.

Holtz, J. (2002). Sensorless control of induction motor drives. In *Proceedings of the IEEE* (Vol. 90(8), pp. 1359–1394).

Hsieh, C.-S. (2003). General two-stage extended Kalman filters. *IEEE Transactions on Automatic Control*, *48*(2), 289–293.

Hsieh, C.-S., & Chen, F.-C. (1999). Optimal solution of the two-stage Kalman estimator. *IEEE Transactions on Automatic Control*, *44*(1), 194–199.

Hurst, K. D., & Habetler, T. G. (1996). Sensorless speed measurement using current harmonic spectral estimation in induction machine drives. *IEEE Transactions on Power Electronics*, *11*(1), 66–73.

Ibarra-Rojas, S., Moreno, J. A., & Espinosa-Pérez, G. (2004). Global observability analysis of sensorless induction motors. *Automatica*, 1079–1085.

Kim, Y.-R., Sul, S.-K., & Park, M.-H. (1994). Speed sensorless vector control of induction motor using extended Kalman filter. *IEEE Transactions on Industry Applications*, *30*(5), 1225–1233.

Leonhard, W. (2001). *Control of electrical drives*. Springer: Springer Verlag.

Marino, R., Tomei, P., & Verrelli, C. (2010). *Induction motor control design*. Springer.

Menaa, M., Touhami, O., Ibtiouen, R., & Fadel, M. (2007). Speed sensorless vector control of an induction motor using spiral vector model-ECKF and ANN controller. In *IEEE international electric machines & drives conference, 2007, IEMDC'07* (Vol. 2, pp. 1165–1170). IEEE.

Petersen, I., & Savkin, A. (1999). *Robust Kalman filtering for signals and systems with large uncertainties*. Boston: Birkhäuser.

Rajashekara, K., Kawamura, A., & Matsuse, K. (1996). *Sensorless control of AC motor drives: Speed and position sensorless operation*. New York: IEEE Press.

Reif, K., Gunther, S., Yaz, E., & Unbehauen, R. (1999). Stochastic stability of the discrete-time extended Kalman filter. *IEEE Transactions on Automatic Control*, *44*(4), 714–728, http://dx.doi.org/10.1109/9.754809.

Rodic, M., & Jezernik, K. (2002). Speed-sensorless sliding-mode torque control of an induction motor. *IEEE Transactions on Industrial Electronics*, *49*(1), 87–95.

Tajima, H., & Hori, Y. (1993). Speed sensorless field-orientation control of the induction machine. *IEEE Transactions on Industry Applications*, *29*(1), 175–180.

Vas, P. (1998). *Sensorless vector and direct torque control*, Vol. 729. Oxford, UK: Oxford University Press.

Yan, Z., Jin, C., & Utkin, V. (2000). Sensorless sliding-mode control of induction motors. *IEEE Transactions on Industrial Electronics*, *47*(6), 1286–1297.